Evidence of a Cationic Substitution Domain in Lithium-Manganese Spinels

C. B. Azzoni, M. C. Mozzati, A. Palearia, V. Massarottib, M. Binib, and D. Capsonib

INFM-Department of Physics "A. Volta" of the University, via Bassi 6, I-27100 Pavia

Z. Naturforsch. 53 a, 771-778 (1998); received June 22, 1998

via Taramelli 16, I-27100 Pavia

Magnetic susceptibility measurements and electron paramagnetic resonance spectra of samples prepared from the reactive system MnO/Li_2CO_3 with different starting Li cationic fraction x are analyzed, taking into account the structural and compositional information provided by x-ray diffraction. Parent phases, as Mn_2O_3 , Mn_3O_4 and Li_2MnO_3 , arise together with the lithium-manganese spinel as a result of Li-deficiency or Li-excess with respect to the x=0.33 composition pertinent to the stoichiometric $LiMn_2O_4$ spinel. The data show that the spinel phase can sustain a partial Li-Mn substitution in the cation sites, according to compositional models described, for x>0.33, by $Li_{1+y}Mn_{1-3y}^{1+}Mn_{1+2y}^{1+}O_4$ (Li-rich spinel) and, for x<0.33, by $Li_{1-|y}|Mn_{1+|y|}^{2+}Mn_{1-|y|}^{3+}Mn_{1-|y|}^{4+}O_4$ (Li-poor spinel). Paramagnetic resonance data of the Li-poor spinel phase are analyzed to discuss the possible oxidation state of Mn in the tetrahedral site.

Key words: Stoichiometric LiMn₂O₄ Spinel Phase, Magnetic Susceptibility, Electron Paramagnetic Resonance.

1. Introduction

Transition metal mixed oxides often exhibit structural, magnetic and transport properties sensibly tunable by small changes of the cation stoichiometry [1]. Lithium manganese spinels are receiving particular attention owing to the coexistence of Mn⁴⁺ and Mn³⁺ valence states [2 - 5]. The magnetic properties of these compounds depend on the Mn oxidation state which may be influenced by a change of the Li cationic fraction. The resulting localization of electrons / holes is important in determining the transport features for possible applications in electrochemistry [6].

Some controversy exists in the literature [2, 7 - 9] on the magnetic susceptibility of the stoichiometric LiMn₂O₄ which shows a sample dependent behaviour, particularly at low temperature. The spread of results may arise from differences in the preparation methods, which can easily introduce unwanted spurious phases [10]. Nevertheless, this fact may also be an evidence of stoichiometry deviations, which

Reprint requests to V. Massarotti; FAX: +39 382 507575, E-mail: vimas@chifis.unipv.it.

may be considerably more interesting for tuning specific physical properties. Indeed, a recent study [11] concerned the effects of oxygen deficiency on the structural phase transition of this compound. By contrast, it is not yet clear whether a not-negligible domain of cationic substitution can exist in the Li-Mn spinel structure.

In this work we present results obtained from the magnetic and diffractometric characterization of samples of Li-Mn oxides prepared by starting from different Li cationic fractions. The identification of the physical features belonging to the spinel phase evidences the existence of both Li-rich and Li-poor spinels. The resulting cationic disproportion gives rise to changes of the relative abundance of different Mn oxidation states.

2. Experimental Procedure

Samples were prepared from starting reacting mixtures MnO/Li_2CO_3 [2, 3] with lithium cationic fraction, x, ranging between 0 and 0.67. The mixtures were previously treated 1 hour at 1073 K (heating rate 5 K/min) to decompose the carbonate and then

0932-0784 / 98 / 0900-0771 \$ 06.00 © Verlag der Zeitschrift für Naturforschung, Tübingen · www.znaturforsch.com



Dieses Werk wurde im Jahr 2013 vom Verlag Zeitschrift für Naturforschung in Zusammenarbeit mit der Max-Planck-Gesellschaft zur Förderung der Wissenschaften e.V. digitalisiert und unter folgender Lizenz veröffentlicht: Creative Commons Namensnennung-Keine Bearbeitung 3.0 Deutschland

This work has been digitalized and published in 2013 by Verlag Zeitschrift für Naturforschung in cooperation with the Max Planck Society for the Advancement of Science under a Creative Commons Attribution-NoDerivs 3.0 Germany License.

^a INFM-Department of Materials Science of the University, via Cozzi 53, I-20126 Milano ^b Department of Physical Chemistry of the University and CSTE-CNR,

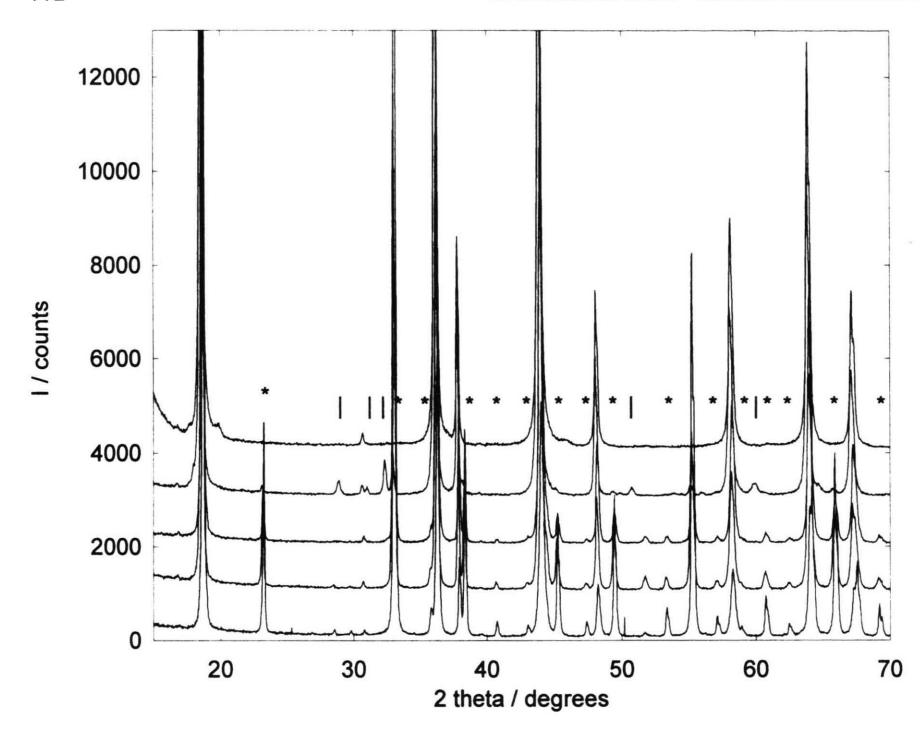


Fig. 1. X-ray powder patterns of samples with x = 0.10, 0.20, 0.25, 0.31 (from the bottom) compared with the pattern of the stoichiometric LiMn₂O₄ sample (upper pattern). Peaks from the Mn₂O₃ and Mn₃O₄ phases are indicated by stars and bars, respectively.

cooled (5 K/min), ground and reheated 8 hours at 1073 K. The stoichiometric sample (x = 0.33) was further reheated to assure the complete transformation of possible impurity phases still present. Other structural phases besides the LiMn2O4 spinel are expected to arise as a result of excess (x > 0.33) or deficiency (x < 0.33) of lithium. So, all the obtained samples were characterized by x-ray diffraction (XRD) in order to identify and quantify the different phases in the samples. Diffraction data were obtained by a Philips PW 1710 powder diffractometer equipped with a Philips PW 1050 vertical goniometer. Use was made of the Cu K α radiation obtained by means of a graphite monochromator. Patterns were collected in the angular range $10^{\circ} < 2\theta < 130^{\circ}$ in step scan mode with a step width of 0.025° and 10 s of counting time. Structural and profile parameters were obtained by the Rietveld refinement procedure [12]. The relative phase amounts were obtained by the procedure of Hill and Howard [13] and corrected for microabsorption effects.

Electron paramagnetic resonance (EPR) measurements were carried out by using a Bruker spectrometer in the X band (9.12 GHz) between 120 and 470 K. The relative spinel phase amounts were estimated by comparing the signal areas with that of pure samples of the coexisting phases, taking particular care

as to the reproducibility of the sample position in the resonant cavity.

Static magnetic susceptibility and magnetization measurements were carried out from 300 down to 4 K, in magnetic fields ranging between 5 and 400 mT, by using a Faraday balance susceptometer with a continuous-flow cryogenic apparatus. The final accuracy of the mass susceptibility $(\chi_{\rm m})$ data results with an error of a few %. The magnetic field dependence was analyzed by changing the field intensity at a fixed temperature.

3. Results

The XRD pattern of $LiMn_2O_4$ (x = 0.33) shows the expected diffraction peaks for the spinel phase.

The x > 0.33 samples show the diffraction lines from both LiMn₂O₄ and Li₂MnO₃ patterns, as previously reported [3, 14]. It was observed that the line shape and broadening are mainly related to the presence of non stoichiometric Li-rich spinel phase [2, 3, 14]. A detailed analysis of the XRD pattern was obtained by considering an effective non-stoichiometry of the spinel phase in addition to the diffraction effects of Li₂MnO₃, in order to determine the phase abundance and composition in the samples from the Rietveld refinement procedure.

Table 1. Sample list: weight % of the indicated phases in samples with different x Li-cationic fraction as determined by XRD, EPR and χ_m measurements. The last two columns show the slopes of $1/\chi_m$ vs. T of the spinel phases (g/cm³K) and the estimated y Li stoichiometry deviation from XRD and EPR data (see text).

\overline{x}	Spinel phase			Mn ₂ O ₃	Mn_3O_4		Li ₂ MnO ₃		1/C _m	\overline{y}
	XRD	EPR	Eqs. (1, 2)	XŘD	XRD	$\chi_{ m m}$	XRD	ÉPR		
0.10	42.4	22	25	57.6	0.0	0.2			30.4	-0.36
0.20	69.5	52	53	30.5	0.0	0.2			31.3	-0.19
0.25	81.0	71	70	19.0	0.0	0.4			31.2	-0.11
0.31	89.0	93	91	3.4	7.6	4.5			33.0	-0.02
0.33	100	100	100						36.7	0
0.36	98.3	98.4	95				1.7	1.6	40.2	0.06
0.40	91.5	92.1	86				8.5	7.9	42.6	0.09
0.44	78.0	81.5	77				22.0	18.5	42.8	0.09
0.53	44.3	58.0	52				55.7	42.0	43.1	0.16

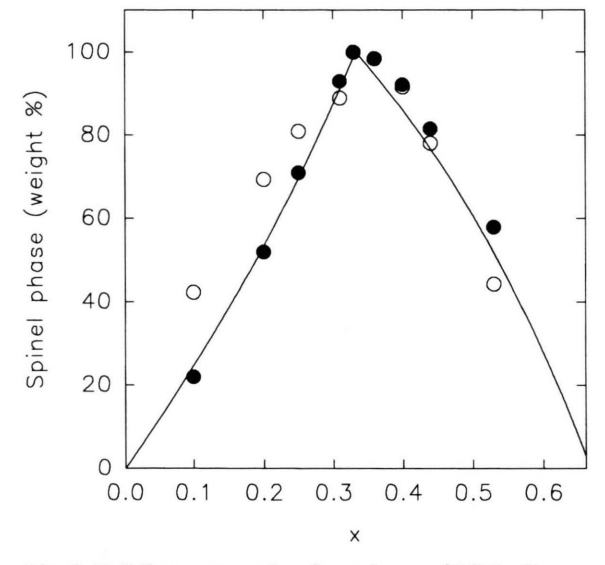


Fig. 2. Full line: expected x-dependence of LiMn₂O₄ mass % in samples with x < 0.33 and x > 0.33 within a purely stoichiometric model, (1, 2). Open circles: values obtained by XRD analysis. Filled circles: values from EPR measurements (see text).

The x < 0.33 samples are characterized by additional lines from $\mathrm{Mn_2O_3}$ and, only in the x = 0.31 sample, from $\mathrm{Mn_3O_4}$, as evidenced by comparing the diffraction profiles in Figure 1. No evidence of a line broadening effect has been observed. Only a slight decrease of the cubic lattice parameter a of the spinel phase has been found with decreasing x but the range of variation of a (between 8.242 Å and 8.234 Å) is much more limited than that previously reported for x > 0.33 samples [14]. In the Rietveld profile analysis, Li $\mathrm{Mn_2O_4}$ and $\mathrm{Mn_2O_3}$ were treated as stoichiometric phases. Table 1 summarizes the complete results of the refinement procedure. The resulting spinel weight

percentages are reported in Fig. 2 and compared with the expected x-dependence of the spinel phase (supposed stoichiometric) amount, $W_{\rm spinel}$, taking into account only the additional ${\rm Mn_2O_3}$ phase for x < 0.33 or the ${\rm Li_2MnO_3}$ phase for x > 0.33:

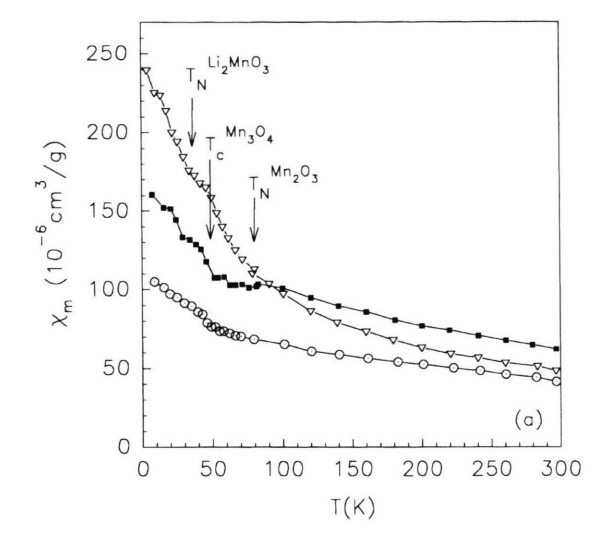
$$W_{\text{spinel}} = 100 \frac{2x M_{\text{spinel}}}{(1 - 3x) M_{\text{Mn}_2\text{O}_3} + 2x M_{\text{spinel}}}$$
 (1)

when x < 0.33,

$$W_{\text{spinel}} = 100 \frac{(3x - 2)M_{\text{spinel}}}{(1 - 3x)M_{\text{Li}_2\text{MnO}_3} + (3x - 2)M_{\text{spinel}}} (2)$$
when $x > 0.33$,

where M_i are the molecular masses.

EPR measurements were carried out on the investigated samples as well as on reference samples of the other phases which accompany the spinel formation. A very broad signal, 300 mT wide with $g \sim 2$ is peculiar of stoichiometric LiMn₂O₄ and is observed in all samples. The signal from Mn₃O₄, 340 mT wide at $g \sim 2$ at 470 K, is quite similar to the broad signal in stoichiometric spinel, except for a temperature dependence of the resonance field. Only a slow shift of the baseline is instead observed in the Mn_2O_3 phase. On the other hand, a well distinct signal arises from Li_2MnO_3 at g = 1.994 with a width of 21 mT, as already described [3]. Comparison of the EPR signal area in the spinel sample (x = 0.33) and in Li₂MnO₃ (containing only Mn⁴⁺ ions), taking into account the respective sample and molecular masses, suggests to assign the spinel broad signal to the Mn⁴⁺ ions only of the LiMn₂O₄ structure. This attribution is consistent with the usually experienced lack of EPR signal from



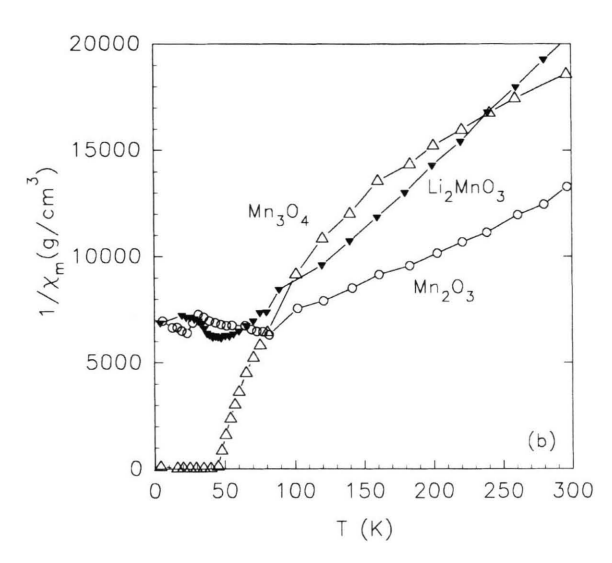


Fig. 3. (a) Mass magnetic susceptibility $\chi_{\rm m}$ of representative samples x=0.25 (squares), x=0.44 (triangles) and stoichiometric x=0.33 (circles). Shoulders due to Mn₂O₃, Mn₃O₄ and Li₂MnO₃ transitions are also indicated (see text). (b) $1/\chi_{\rm m}$ data of Mn₂O₃, Mn₃O₄ and Li₂MnO₃ are reported for comparison.

Mn³⁺ ions, also supported by theoretical argumentations [15].

As a result of the EPR features just described, samples with x < 0.33 do not show peculiar features from the amounts of Mn_2O_3 and Mn_3O_4 revealed by XRD. Only minor intensity contributions from the Mn_3O_4 signal are to be taken into account (by subtracting the Mn_3O_4 signal weighted for the pertinent phase amount) in order to analyze the EPR response of the

spinel phase alone. In samples with x > 0.33 the well distinct signal of Li_2MnO_3 allowed us to determine by subtraction the amount of spinel phase with high accuracy. The weight % of the spinel phase evaluated in all samples is reported in Table 1. These values follow the x-behaviour described by (1) within the experimental errors in samples with x < 0.33, while they are above the theoretical curve (2) in samples with x > 0.33 (see Figure 2).

In Fig. 3a, mass susceptibility (χ_m) vs. temperature curves of representative samples are reported and compared with data of a sample of stoichiometric LiMn₂O₄ spinel. The features at about 80, 45 and 35 K can be well accounted for by the presence of the other phases identified by XRD analysis. As evidenced in Figure 3b, where the $1/\chi_{\rm m}$ curves of ${\rm Mn_2O_3}$, ${\rm Mn_3O_4}$ and Li₂MnO₃ pure samples are reported for comparison, the shoulder at 80 K, observed in samples with x < 0.33, corresponds to the maximum of the Mn₂O₃ susceptibility at the antiferromagnetic transition at T = 80 K, and the rise of χ_{m} just below 50 K to the ferrimagnetic transition of Mn_3O_4 at T = 49 K. Similarly, the flexion below 40 K in samples with x > 0.33can be attributed to the antiferromagnetic transition of Li₂MnO₃ at 35 K. By contrast, the change in the slope at about 40 K in the $\chi_{\rm m}$ curve of the stoichiometric spinel, also observed by other authors [11], cannot be reasonably assigned to spurious phases, but probably indicates the onset of antiferromagnetic ordering [16]. Note that the presence of Mn₃O₄ in samples with x < 0.33 is not revealed by XRD except for the x = 0.31 sample. This may happen because the Mn₃O₄ amount is below the XRD detection limit. In fact, the interpolation at zero field of magnetization curves taken below 50 K shows the presence of non-zero spontaneous magnetization M(0) consistent with weight concentrations of ferrimagnetic Mn₃O₄ of only few ‰ (see Table 1).

In order to analyze the magnetic behaviour of only the Li-Mn spinel phase in samples produced in conditions of Li-excess or Li-deficiency, susceptibility data were corrected for additive contributions from different phases according to the phase percentages estimated by XRD and EPR analysis or magnetization measurements (for $\mathrm{Mn_3O_4}$). Figure 4 shows the temperature behaviour in the paramagnetic region of the $1/\chi_{\mathrm{m}}$ values so obtained. The corrected data follow a linear temperature dependence above $100~\mathrm{K}$, according to the Curie-Weiss behaviour $(T-\theta)/C_{\mathrm{m}}$. But a remarkable result emerges from this analysis:

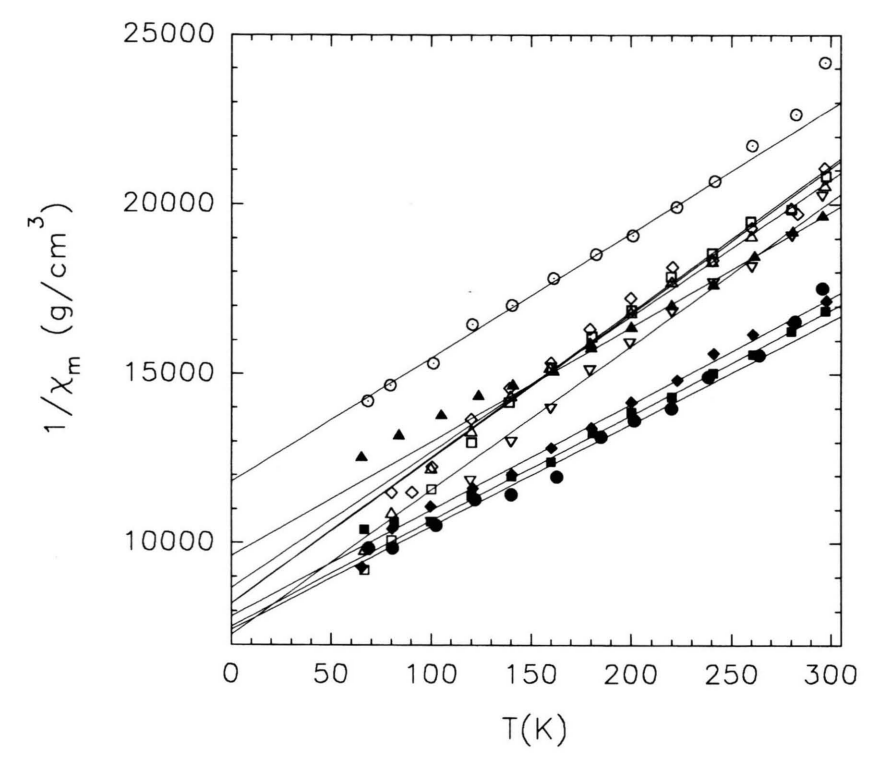


Fig. 4. $1/\chi_{\rm m}$ data of the spinel phase in the paramagnetic region: (filled marks) data from samples with x < 0.33 (x = 0.10 circles; x = 0.20 diamonds; x = 0.25 squares; x = 0.31 triangles); (open marks) data from samples with x > 0.33 (x = 0.36 triangles up; x = 0.40 triangles down; x = 0.44 squares; x = 0.53 diamonds) and stoichiometric sample (open circles). The linear regressions of the paramagnetic behaviour are also shown.

the average behaviour found in samples with x > 0.33 differs from those with x < 0.33, and both are different from that of stoichiometric $\operatorname{LiMn_2O_4}$. Specifically, the $1/\chi_{\rm m}$ curves of the spinel phase in samples with x > 0.33 are characterized by higher slopes (lower Curie constant $C_{\rm m}$), while lower slopes (higher $C_{\rm m}$ constant) are observed in the spinel phase of samples with x < 0.33. This fact is better evidenced by the linear interpolation of the data (full lines in Figure 4). Some effects also exist in the intercepts on the temperature axis (the θ constant), since samples with x > 0.33 (-215 K < θ < -170 K) and x < 0.33 (-285 K < θ < -240 K) show absolute θ values which are lower than that observed in the spinel phase ($\theta \cong -320$ K).

4. Discussion

In previous papers we suggested the presence of Li-rich Li-Mn spinel phases describable as $\operatorname{Li}_{1+y}\operatorname{Mn}_{2-y}\operatorname{O}_4$ from joined XRD and EPR investigation of samples with x > 0.33 [2, 3]. In the present work we analyze the non-stoichiometry of Li-Mn spinel phases produced by starting both with Liexcess and Li-deficiency.

The data of samples with x < 0.33 starting from XRD results will be discussed first. The observed

excess of the spinel phase with respect to that expected from (1) (Fig. 2) suggests the following models:

- A) creation of Li vacancies in the Li-Mn spinel structure together with the formation of Mn oxides;
- B) formation of a Li-poor spinel phase by partial substitution of Li by Mn ions, along with the formation of Mn oxides.

Both cases, involving two types of Li-poor spinel structures, can account for the excess of spinel phase with respect to the expected amount of stoichiometric phase.

The present magnetic results suggest to reject the occurrence of Li vacancies (situation A). In fact, the requirement of charge neutrality should lead to a disproportion of the Mn⁴⁺/Mn³⁺ ratio favouring Mn⁴⁺ ions, or to the formation of oxygen vacancies which would keep unchanged the Mn⁴⁺/Mn³⁺ ratio. Both these models clash with the susceptibility data in Figure 4. Actually, the $C_{\rm m}$ values of the spinel phase in samples with x < 0.33 are higher than the value of the stoichiometric spinel, thus suggesting that the effective magnetic moment

$$m_{\rm eff} = \sqrt{\frac{3k_{\rm B}}{N_{\rm A}\mu_{\rm B}^2}} \frac{M}{n} C_{\rm m} \tag{3}$$

is higher than that expected if the Mn⁴⁺/Mn³⁺ ratio were the same or higher with respect to the stoichiometric spinel, since the Mn³⁺ and Mn⁴⁺ spin-only magnetic moments are 4.9 $\mu_{\rm B}$ and 3.9 $\mu_{\rm B}$, respectively. In (3) $k_{\rm B}$, $N_{\rm A}$ and $\mu_{\rm B}$ are respectively the Boltzmann constant, the Avogadro number and the Bohr magneton, while M is the molecular mass of the compound and n is the effective number of Mn ions per formula unit (n =2 in stoichiometric LiMn₂O₄).

Therefore, one is forced to consider the existence of Li-poor spinel phases arising from cationic substitution of lithium by Mn ions (situation B). Similarly, as regards the samples with x > 0.33, the EPR and XRD data in Fig. 2 and the low $m_{\rm eff}$ values from $1/\chi_{\rm m}$ curves of Fig. 4 confirm the substitution of Mn by Li in the octahedral site, as already described [2, 3].

The extent of the Li stoichiometry deviation y in the spinel phase can be estimated by comparing the $m_{\rm eff}$ values from $1/\chi_{\rm m}$ data with the y-dependence of the magnetic moment. So, the cationic substitution ${\rm Li}_{1+y}{\rm Mn}_{2-y}{\rm O}_4$ (with y>0 in Li-rich spinel and y<0 in Li-poor spinel) must be made explicit in terms of the different Mn oxidation states. In the case of Li enrichment, the different Mn oxidation states can be reliably described [3] as

$$\text{Li}_{1+y}\text{Mn}_{1-3y}^{3+}\text{Mn}_{1+2y}^{4+}\text{O}_4.$$
 (4)

On the other hand, in Li-poor spinel, two models may be considered: a) substitution of lithium by Mn²⁺ ions, b) substitution of lithium by Mn³⁺ ions, respectively, described by

$$\text{Li}_{1-|y|}\text{Mn}_{|y|}^{2+}\text{Mn}_{1+|y|}^{3+}\text{Mn}_{1-|y|}^{4+}\text{O}_4,$$
 (5)

$$\text{Li}_{1-|y|}\text{Mn}_{1+3|y|}^{3+}\text{Mn}_{1-2|y|}^{4+}\text{O}_{4}.$$
 (6)

Equation (5) is consistent with the limit parent phase (for y = -1) $\mathrm{Mn_3O_4}$ which is a spinel with $\mathrm{Mn^{3+}}$ ions in octahedral site and $\mathrm{Mn^{2+}}$ in tetrahedral site (the Li site of the $\mathrm{LiMn_2O_4}$ spinel). Equation (6) is the symmetric extension of the cationic substitution already proposed for Li-enrichment, (4). Anyway, taking into account the influence of y on the effective number of Mn ions per formula unit and on the molecular mass, the effective magnetic moment can be expressed as

$$m_{\rm eff} = \sqrt{\frac{3k_{\rm B}}{N_{\rm A}\mu_{\rm B}^2}} \frac{M(1-Dy)}{2-y} C_{\rm m},$$
 (7)

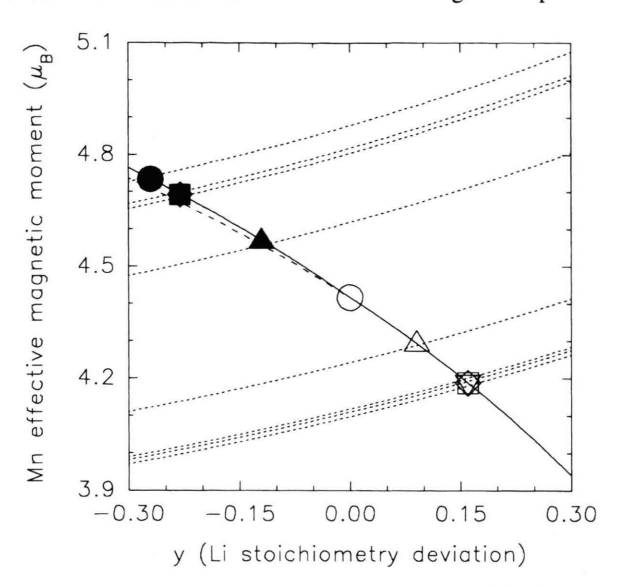


Fig. 5. Intersection of the curves derived from (8,9) (continuous lines) and from (10) (long-dashed line) with the curves obtained from (7) (short-dashed lines) for each experimental $C_{\rm m}$ value (symbols as in Figure 4).

where D is the difference between the atomic mass of Mn and Li divided by the molecular mass M of the stoichiometric $\operatorname{LiMn_2O_4}$. By inserting the experimental C_{m} values into (7), one obtains a $m_{\mathrm{eff}}(y)$ function for each investigated sample (short-dashed lines in Figure 5). Equation (7) can be used to estimate the Li-deficiency and Li-enrichment of the spinel phase. Indeed, the y values may be derived by solving the system formed by (7) and the theoretical expressions calculated (in the spin-only limit) according to the compositional models in (4 - 6):

$$m_{\text{eff}}^2 = \frac{1}{2 - y} \left[(1 - 3y) m_{\text{Mn}^{3+}}^2 + (1 + 2y) m_{\text{Mn}^{4+}}^2 \right],$$
 (8)

$$m_{\text{eff}}^2 = \frac{1}{2 + |y|} \left[|y| m_{\text{Mn}^{2+}}^2 + (1 + |y|) m_{\text{Mn}^{3+}}^2 + (1 - |y|) m_{\text{Mn}^{4+}}^2 \right], \tag{9}$$

$$m_{\rm eff}^2 = \frac{1}{2 + |y|} \left[(1 + 3|y|) m_{\rm Mn^{3+}}^2 + (1 - 2|y|) m_{\rm Mn^{4+}}^2 \right]. (10)$$

Equation (8) (valid for y > 0) and (9) and (10) (for y < 0 in the case a) and b) respectively) follow from the additive property of the mass susceptibility, which is proportional to $m_{\rm eff}^2$. All these theoretical behaviours are shown in Fig. 5 [continuous lines for (8, 9) and

dashed line for (10)]. Intersections of the curves derived from (8 - 10) with the curves obtained from (7) (short-dashed lines) occur in the range -0.3 < y < -0.1 in Li-poor spinels (both for Mn²⁺ and Mn³⁺ Li-substitution) and 0.1 < y < 0.2 in Li-rich spinels. Taking into account the errors in the $m_{\rm eff}$ estimation procedure, the y values so obtained agree well with those calculated within the present compositional model, (4 - 6), by comparing the experimental spinel phase amounts (obtained by XRD for x < 0.33 and by EPR for x > 0.33) with those derived from the purely stoichiometric prediction (1, 2) and reported in Table 1.

However, we have no means to discriminate from susceptibility or XRD data which type of Li-substitution occurs in Li-poor spinel, i. e. Mn²⁺ or Mn³⁺ in Li sites [(5, 9) or (6, 10), respectively]. Aid in this respect may come from EPR data. In fact, EPR signals from the Li-poor spinel phase can only arise from Mn⁴⁺ in octahedral site and Mn²⁺ or Mn³⁺ in tetrahedral site, since no EPR signal is expected from Mn³⁺ ions in octahedral site. However, Mn³⁺ ions in tetrahedral site should not be EPR active since the spin levels splitting caused by the spin-orbit interaction leads to a singlet ground state with an energy separation from the first excited spin level much larger than the microwave energy $h\nu$. So, model b) implies that the EPR signal arises from only 1 - 2|y| Mn⁴⁺ ions per formula unit. But in this case the Li-poor spinel percentage should be 1/(1-2|y|) times that estimated by supposing the EPR signal as arising from stoichiometric spinel (data in Figure 2). The W_{spinel} values so obtained are too high and not consistent with the x Li cationic fraction. In the model a), Mn²⁺ ions in tetrahedral sites are expected to contribute with an EPR signal of the same type as that observed in Mn₃O₄, whose area is indeed consistent with its attribution to only Mn²⁺ ions. This signal is very similar to that observed in stoichiometric spinel, and its presence in Li-poor spinel would not be discernible from that arising from Mn⁴⁺ ions in octahedral sites. In this case, one should expect a negligible y-dependence of the EPR spinel signal because of the compensating contributions (1 - |y|)and |y| from Mn⁴⁺ and Mn²⁺ ions respectively, (5). So the x-dependence of the EPR signal of Li-poor spinel should be the same as that expected in the case of stoichiometric spinel, in agreement with the data in Fig. 2. Therefore, the most probable picture should consider Li sites progressively substituted by Mn^{2+} ions on decreasing x.

It can be pointed out that the spinel phase prepared by our reactive system is substantially a substitutional cationic compound, clearly distinct from spinels such as $\text{Li}_2\text{Mn}_4\text{O}_9$ ($\text{Li}_{1-\delta}$ $\text{Mn}_{2-2\delta}\text{O}_4$) which possess Li and Mn vacancies [8, 17]. The investigated samples are also to be distinguished from the substitutional spinel $\text{Li}_4\text{Mn}_5\text{O}_{12}$ ($\text{Li}_{1+\delta}\text{Mn}_{2-\delta}\text{O}_4$) [8, 17, 18] which contains only Mn^{4+} ions and is characterized by ferromagnetic behaviour [8].

5. Conclusions

Detailed consideration of XRD, $\chi_{\rm m}$ and EPR data on Li-Mn spinels, prepared from the reactive system MnO/Li₂CO₃ with Li-excess and Lideficiency, shows the occurrence of cationic substitution. A satisfactory description of the experimental results can be achieved by means of the compositional models $\text{Li}_{1+y}\text{Mn}_{1-3y}^{3+}\text{Mn}_{1+2y}^{4+}\text{O}_4$ and $\mathrm{Li}_{1-|y|}\mathrm{Mn}_{|y|}^{2+}\mathrm{Mn}_{1+|y|}^{3+}\mathrm{Mn}_{1-|y|}^{4+}\mathrm{O}_4$ for Li-rich and Lipoor spinel, respectively. In other words, our spinel phases are purely substitutional phases while no evidence is found of vacancy defective spinels as usually obtained by electrochemical methods or low temperature synthesis [8, 17, 18]. In phase-diagram representation, our spinels - from high temperature solid state synthesis - lie in compositional ranges delimited by the triangles LiMn₂O₄-LiMnO₂-Mn₃O₄ and LiMn₂O₄-Li₂MnO₃-Li₄Mn₅O₁₂ (in the cases of Lipoor and Li-rich samples, respectively). Our results show that some of the limiting phases are absent, suggesting their instability in the thermodynamic conditions of the reactive system.

Acknowledgements

This work has been partially funded by Consorzio per i Sistemi a Grande Interfase (CSGI) and by Progetto Finalizzato MSTA II of CNR.

- V. Massarotti, D. Capsoni, M. Bini, C. B. Azzoni, M. C. Mozzati, and A. Paleari, Z. Naturforsch. 53a, 150 (1998).
- [2] V. Massarotti, D. Capsoni, M. Bini, G. Chiodelli, C.B. Azzoni, M. C. Mozzati, and A. Paleari, J. Solid State Chem. 131, 94 (1997).
- [3] V. Massarotti, D. Capsoni, M. Bini, C.B. Azzoni, and A. Paleari, J. Solid State Chem. 128, 80 (1997).
- [4] A. Yamada and M. Tanaka, Mat. Res. Bull. 30, 715 (1995).
- [5] A. Yamada, J. Solid State Chem. 122, 160 (1996).
- [6] J. M. Tarascon, W. R. McKinnon, F. Coowar, T. N. Bowmer, G. Amatucci, and D. Guyomard, J. Electrochem. Soc. 141, 1421 (1994).
- [7] J. Sugiyama, T. Tamura, and H. Yamauchi, J. Phys.: Condens. Matter 7, 9755 (1995).
- [8] C. Masquelier, M. Tabuchi, K. Ado, R. Kanno, Y. Kobayashi, Y. Maki, O. Nakamura, and J. B. Goodenough, J. Solid State Chem. 123, 255 (1996).
- [9] N. Kumagai, T Fujiwara, K. Tanno, and T. Horiba, J. Electrochem. Soc. 143, 1007 (1996).

- [10] C. B. Azzoni, M. C. Mozzati, A. Paleari, V. Massarotti, D. Capsoni, and M. Bini, Z. Naturforsch. 53a (1998) in the press.
- [11] J. Sugiyama, T. Atsumi, A. Koiwai, T. Sasaki, T. Hioki, S. Noda, and N. Kamegashira, J. Phys.: Condensed Matter 9, 1729 (1997).
- [12] H. M. Rietveld, J. Appl. Crystallogr. 2, 65 (1969).
- [13] R. J. Hill and C. J. Howard, J. Appl. Crystallogr. 20, 467 (1987).
- [14] V. Massarotti, M. Bini, and D. Capsoni, Z. Naturforsch. 51a, 267 (1996).
- [15] C. B. Azzoni, M. Catti, A. Paleari, and C. Pogliani, J. Phys.: Condensed Matter 9, 3931 (1997).
- [16] J. Sugiyama, T. Hioki, S. Noda, and M. Kontani, J. Phys. Soc. Japan 66, 1187 (1997).
- [17] R. J. Gummow, A. deKock, and M. M. Thackeray, Solid State Ionics 69, 59 (1994).
- [18] T. Takada, E. Akiba, F. Izumi, and B. C. Chakownakos, J. Solid State Chem. 130, 74 (1997).